

Strange hadron production in Au+Au collisions at $\sqrt{s_{NN}} = 3 - 27$ GeV with UrQMD

A. Timofeev^{a,b,1}, A. Korobitsin^{a,2}

^a Joint Institute for Nuclear Research, Dubna, Russia, 141980

^b Lomonosov Moscow State University, Moscow, Russia, 119991

We study model dependence of strange hadron spectra (K_S^0 , Λ , Ξ , Ω) on transverse momentum, rapidity, and collision centrality in Au+Au collisions in the range of energies $\sqrt{s_{NN}} = 3 - 27$ GeV using the UrQMD model. The results are compared with the data from RHIC Beam Energy Scan (BES) program. While the model shows reasonable agreement for K_S^0 spectra, it systematically underestimates the yields of strange and multi-strange hadrons over the entire energy range, with the discrepancy increasing with the strangeness content. The antibaryon-to-baryon and hadron-to-pion ratios are qualitatively reproduced, but significant quantitative deviations persist. These results demonstrate that, in its present form, the UrQMD model does not provide a satisfactory description of strange hadron observables at $\sqrt{s_{NN}} = 3 - 27$ GeV, indicating the need for additional physical mechanisms beyond hadronic rescattering to account for strangeness production in high-density nuclear matter.

PACS: 14.20.Jn, 14.40.-n

Introduction

The study of strongly interacting matter under extreme conditions of high temperature and baryon density is a central goal of relativistic heavy-ion collisions. Quantum Chromodynamics (QCD) predicts the phase transition from a state of confined hadrons to a deconfined Quark-Gluon Plasma (QGP). The investigation of the phase diagram of QCD, particularly locating the critical point and the phase boundary between hadronic matter and QGP, remains a major challenge in the field [1].

Strange hadrons are considered as an exceptional probes for this endeavor. As the strangeness is not contained in the initial colliding nuclei, all strange particles are entirely produced by the strange quarks occurring during the collision dynamics and possible QGP phase. Therefore, a drastic change in the total yields of strange particles is considered as a signature of the transition to the partonic phase of nuclear matter. In particular, the enhancement of strange hadron production in heavy-ion collisions with respect to proton collisions has been proposed as a signature of QGP formation [2], and their study across a wide collision energy range is essential for identifying the phase boundary and the onset of deconfinement.

¹E-mail: timofeev@jinr.ru

²E-mail: koroaa@jinr.ru

Among the most informative observables are the ratios of strange baryons to mesons (Ξ/π , Λ/π) and antibaryons to baryons ($\bar{\Xi}/\Xi$, $\bar{\Lambda}/\Lambda$). These ratios provide a tool for a more precise determination of phase transition energy and its characteristics. A systematic measurement of the ratios energy dependence across the range of the Beam Energy Scan (BES) program at the Relativistic Heavy Ion Collider (RHIC) can help better localize the phase boundary in the produced medium.

In this context, the comparison between experimental data and theoretical models is important. Discrepancies between the experiment and transport models, such as the Ultra-relativistic Quantum Molecular Dynamics (UrQMD) model [3], which simulates collisions as a sequence of hadron scattering processes without a phase transition to QGP, can reveal the onset of a deconfined state or changes in hadronization processes. In this work, we present the results of the production of strange hadrons in Au+Au collisions at the $\sqrt{s_{NN}} = 3-27$ GeV obtained from the UrQMD model (Cascade mode, EoS = 0), compared to BES phase I (BES-I) data. Furthermore, we investigate the kinematics of strange particles near the production threshold at the lowest BES-II energies.

Experimental setup and analysis details

Data on Au+Au collisions for $\sqrt{s_{NN}} = 7.7, 11.5, 19.6$ and 27 GeV used for current analysis were collected during the BES-I program by STAR experiment in 2010 and 2011. A detailed description of STAR detector can be found in [4]. The main subdetectors used in the analysis of particle production were the Time Projection Chamber (TPC), which covers 2π azimuthal angle in the transverse to the beam direction and from -1 to 1 in pseudorapidity η [5] and Time-of-Flight (TOF) system [6]. Charged particles were identified by their ionization energy loss in the TPC $\langle dE/dx \rangle$ in momentum range from 0.1 GeV/c and by the relative velocity of the track in TOF in momentum range from 0.4 GeV/c. For the reconstruction of the secondary vertex of strange particles (K_S^0 , Λ , Ξ , Ω) charged π , K , p tracks were used.

Particle spectra and yields

Figure 1 demonstrates p_T spectra of K_S^0 , Λ , $\bar{\Lambda}$, Ξ^- , $\bar{\Xi}^+$, Ω^- , $\bar{\Omega}^+$ particles at mid-rapidity ($|y| < 0.5$) for Au+Au collisions at $\sqrt{s_{NN}} = 27$ GeV at different centralities produced with the UrQMD Monte Carlo model. It shows characteristic exponential behavior for strange hadrons. The UrQMD spectra for K_S^0 demonstrate a similarity to the BES-I data [7] for $p_T \lesssim 1$ GeV/c, while a different slope can be observed for $p_T \gtrsim 1$ GeV/c at all centralities. However, for all strange baryons (Λ , $\bar{\Lambda}$, Ξ^- , $\bar{\Xi}^+$, Ω^- , and $\bar{\Omega}^+$), we found that UrQMD significantly underestimates the total yields at all centralities.

While the total yields (dN/dy) for K_S^0 in UrQMD are close to the experimentally measured value, the model systematically underestimates the total

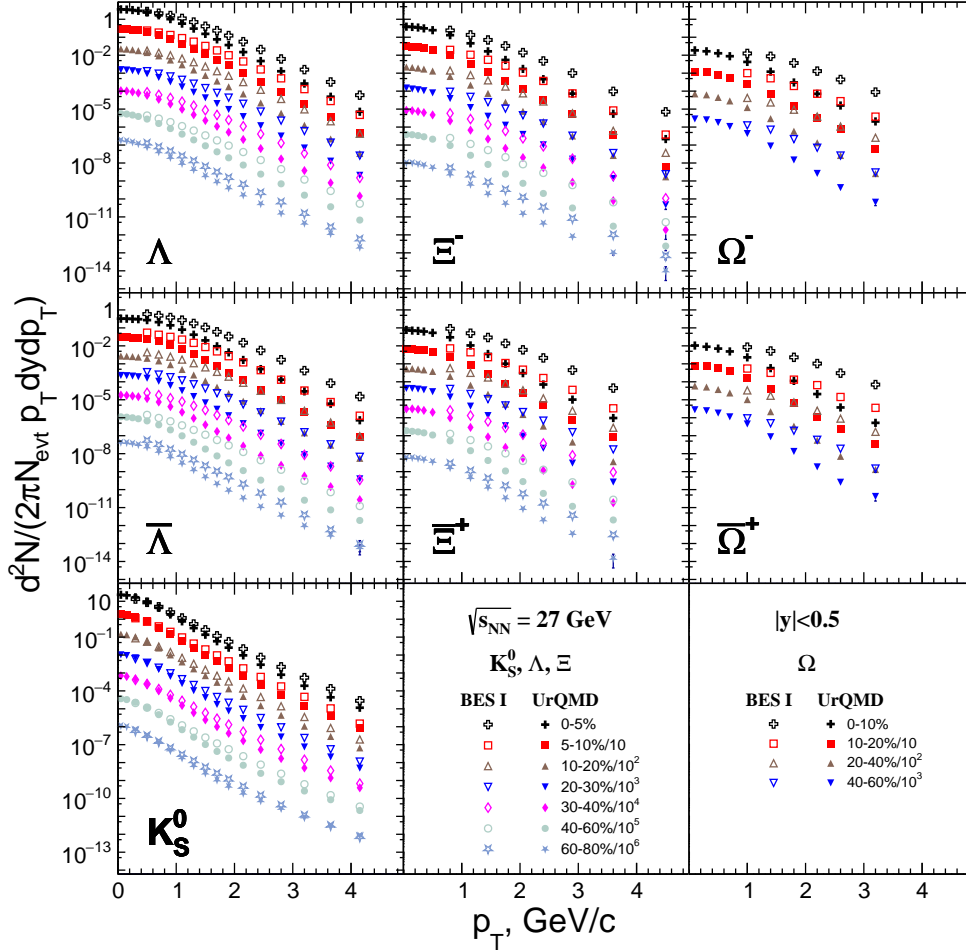


Figure 1. The transverse momentum spectra at mid-rapidity for strange hadrons from Au+Au collisions at 27 GeV energy at different centralities. The data points are scaled for clarity by factors of 10 from central to peripheral collisions. The solid symbols are UrQMD calculations, and open symbols are BES-I data [7].

67 yields of Λ and Ξ for all centralities at mid-rapidity, and the suppression is
 68 particularly noticeable for multi-strange Ξ baryons. This behavior for Λ and
 69 Ξ is observed for all energies from 7.7 to 27 GeV. However, the shape of the
 70 energy dependence of the particle yields is similar to the world data from
 71 central Au+Au collisions from BES-I [7], AGS [9,10], and in Pb+Pb central
 72 collisions at NA49 [11]. Thus, it indicates that the strangeness enhancement
 73 effect cannot be described solely by hadronic re-scattering.

74 Antibaryon-to-baryon ratio

75 The antibaryon-to-baryon ratios are sensitive to net-baryon density in the
 76 collision region and provide insight into baryon transport number. Figure 2
 77 presents the centrality dependence of the $\bar{\Lambda}/\Lambda$ and Ξ^+/Ξ^- at 7.7 and 27
 78 GeV at mid-rapidity, as well as the energy dependence for central collisions.

79 The BES-I data [7] show that ratios decrease from peripheral to central
 80 collisions, reflecting the increased net-baryon density. While the UrQMD
 81 model exhibits the same trend, a quantitative discrepancy is observed. In
 82 central collisions, UrQMD underestimates \bar{B}/B ratios for $\sqrt{s_{NN}} = 7.7 - 27$
 83 GeV. In peripheral collisions, UrQMD overestimates $\bar{\Xi}^+/\Xi^-$ at all energies
 84 across $7.7 - 27$ GeV, overestimates $\bar{\Lambda}/\Lambda$ at 7.7 GeV, and underestimates at
 85 27 GeV.

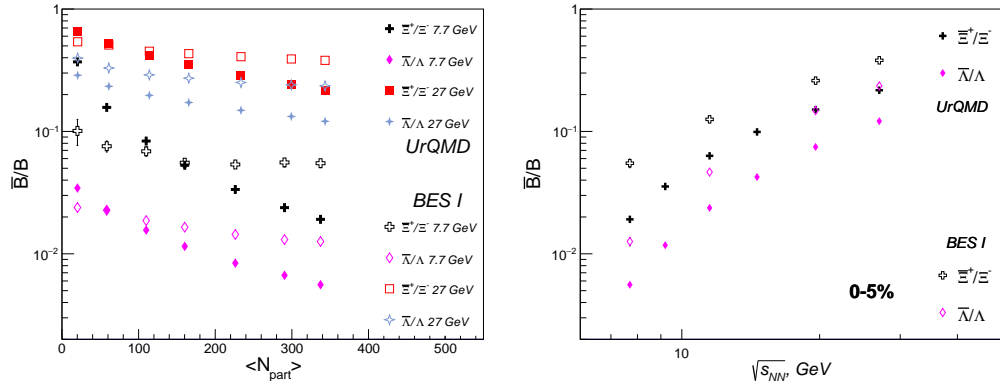


Figure 2. The antibaryon to baryon ratio at mid-rapidity as function of $\langle N_{part} \rangle$ for 7.7 and 27 GeV energies (left plot) and as a function of $\sqrt{s_{NN}}$ for most central collisions (right plot). The solid symbols are UrQMD data, and open symbols are BES-I data [7].

Hadron-to-pion ratios

86
 87 The mid-rapidity Λ , $\bar{\Lambda}$, Ξ^- , and $\bar{\Xi}^+$ yields to the total pions ($1.5(\pi^+ + \pi^-)$)
 88 yield ratios for the most central collisions, calculated with UrQMD, are pre-
 89 sented in Figure 3. The Λ/π and Ξ^-/π ratios demonstrate a monotonic
 90 decrease starting from ≈ 4.5 GeV and ≈ 5.2 GeV, respectively. In contrast,
 91 $\bar{\Lambda}/\pi$ and $\bar{\Xi}^+/\pi$ exhibit a monotonic growth across the energy range from 3
 92 to 27 GeV. These trends are in qualitative agreement with world data from
 93 STAR [7, 8], AGS [9, 10, 12], and NA49 [11] experiments, while the absolute
 94 values of the ratios are suppressed in the model.

95 The K^+/π^+ ratio from UrQMD at mid-rapidity as a function of energy for
 96 central collisions shows a smooth peak approximately at 4.5 GeV while the ex-
 97 perimental data [8] demonstrate a sharp peak (usually called the "horn"-like
 98 effect) at 7.7 GeV. In the K^-/π^- ratio, UrQMD reproduces the experimen-
 99 tally observed trend of a monotonic rise with increasing collision energy.

Near the threshold production

100
 101 The study of strange hadrons at collision energies close to their kine-
 102 matic threshold is a unique probe into the role of multi-nucleon interactions

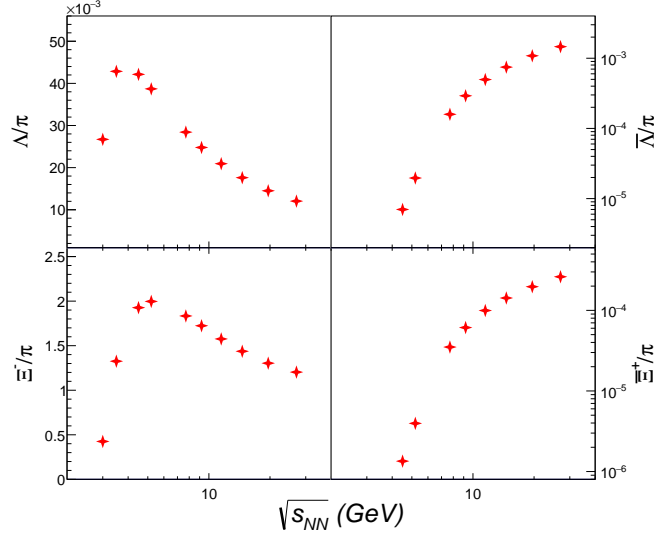


Figure 3. The Λ , $\bar{\Lambda}$, Ξ^- , $\bar{\Xi}^+$ to pions ($1.5(\pi^+ + \pi^-)$) ratios energy dependence at mid-rapidity for 0 – 5% centrality

and the properties of high baryon density matter. The production of multi-strange hyperons is particularly compelling near the threshold [13], where the available phase space is constrained.

We analyze the fraction R of strange hadrons produced in the region of phase volume forbidden in the $p + p$ collisions region (cumulative region) and falling within the STAR acceptance ($-2 < \eta < 0$) to the total yield of particles of a given type. For Au+Au collisions at $\sqrt{s_{NN}} = 3$ GeV, the value of R is remarkably high: 0.73 for Ξ^- , 0.43 for K_S^0 , and 0.38 for Λ . This indicates that a significant part of strange particles is produced in the experimentally achieved cumulative region.

The exceptionally high R value for Ξ^- at $\sqrt{s_{NN}} = 3$ GeV demonstrates its sensitivity to multi-nucleon correlations, consistent with the observed centrality dependence of Ξ^- production at near-threshold energies [13–15]. At $\sqrt{s_{NN}} = 4.5$ GeV the value of R decreases sharply (e.g. $R_{\Xi^-} \approx 0.10$).

Conclusions

The UrQMD model calculations were compared with the experimental data on strange hadron production in Au+Au collisions at $\sqrt{s_{NN}} = 3 - 27$ GeV. The model shows agreement with K_S^0 production but significantly underestimates the yield of strange baryons, with the discrepancy increasing with strangeness content. The antibaryon-to-baryon ratios ($\bar{\Lambda}/\Lambda$, $\bar{\Xi}^+/\Xi^-$) demonstrate centrality dependent discrepancies: UrQMD model underestimates ratios in central collisions and overestimates them in peripheral collisions. While the model reproduces general trends for the hadron-to-pion ratios (Λ/π , Ξ/π , K^-/π^-), it fails to describe a "horn"-like effect in the K^+/π^+ ratio observed in the experiment.

Similar discrepancies between transport model calculations and experimental measurements of strange hadron production have been reported in comparisons with other microscopic approaches. Studies comparing HSD and PHSD calculations with NA49 and NA57 data show that purely hadronic transport models tend to underestimate strange baryon yields, while hybrid approaches including partonic phases improve the description only partially [16]. Comparisons of the AMPT model with NA49 and NA57 measurements further reveal a systematic underestimation of hadron yields and overestimation of antihyperon production [17]. Together with the present UrQMD results, these findings indicate that the observed discrepancies are not model-specific but reflect a more general challenge for transport models in describing strangeness production and baryon–antibaryon dynamics at BES energies. The systematic deviations observed over the wide energy range $\sqrt{s_{NN}} = 3 - 27$ GeV point to the importance of medium-induced effects in high baryon density matter, such as modified string fragmentation, collective multi-string interactions, or changes in hadron masses and production thresholds related to partial chiral symmetry restoration, which are beyond the scope of the current UrQMD implementation.

In addition, the analysis of strange hadron production near the kinematic threshold shows that at low collision energies ($\sqrt{s_{NN}} \lesssim 4$ GeV) a substantial fraction of strange particles originates from the cumulative region, indicating an enhanced role of multi-nucleon interactions and high baryon density effects. In this near-threshold regime, strangeness production becomes particularly sensitive to the treatment of multi-particle dynamics and medium effects, which are only effectively implemented in purely hadronic transport models such as UrQMD. As a result, these observations provide an additional indication of the limitations of the current UrQMD approach in describing strangeness production under extreme density conditions.

Funding

This research was supported by Russian Science Foundation grant number 22-72-10028-II.

Conflict of interest

The authors declare that they have no conflict of interest.

References

1. *Stephanov, M. A.* QCD PHASE DIAGRAM AND THE CRITICAL POINT // International Journal of Modern Physics A — 2005. — V. 20, no. 19. — P. 4387-4392.

- 165 2. *Rafelski, J. and Müller, B.* Strangeness Production in the Quark-Gluon
166 Plasma // Phys. Rev. Lett. — 1982. — V. 48. — P. 1066-1069.
- 167 3. *Bass S.A., Belkacem M., Bleicher M., Brandstetter M., Bravina L., et al.*
168 Microscopic models for ultrarelativistic heavy ion collisions // Progress in
169 Particle and Nuclear Physics — 1998. — V. 41. — P. 255-369.
- 170 4. *Ackermann K. et al.* [STAR collaboration] STAR detector overview //
171 Nucl. Instrum. Meth. A — 2003. — V. 499. — P. 624-632.
- 172 5. *M. Anderson, J. Berkovitz, W. Betts, et al* The STAR time projection
173 chamber: a unique tool for studying high multiplicity events at RHIC //
174 Nucl. Instrum. Meth. A — 2003. — V. 499. — P. 659-678.
- 175 6. *W. J. Llope, F. Geurts, J. W. Mitchell, Z. Liu, N. Adams, et al.* The
176 TOFp / pVPD time-of-flight system for STAR // Nucl. Instrum. Meth.
177 A — 2004. — V. 522. — P. 252-273.
- 178 7. *J. Adam et al.* [STAR collaboration] Strange hadron production in Au+Au
179 collisions at $\sqrt{s_{NN}} = 7.7, 11.5, 19.6, 27, \text{ and } 39 \text{ GeV}$ // Phys. Rev. C —
180 2020. — V. 102. — P. 034909.
- 181 8. *L. Adamczyk et al.* [STAR collaboration] Bulk properties of the medium
182 produced in relativistic heavy-ion collisions from the beam energy scan
183 program // Phys. Rev. C — 2017. — V. 96. — P. 044904.
- 184 9. *S. Ahmad, B.E. Bonner, C.S. Chan, et al.* Λ production by 11.6 A GeV/c
185 Au beam on Au target // Phys. Lett. B — 1996. — V. 382. — P. 35-39.
- 186 10. *B. B. Back et al.* [E917 collaboration] Antilambda Production in $Au +$
187 Au Collisions at 11.7A GeV/c // Phys. Rev. Lett. — 2001. — V. 87. —
188 P. 242301.
- 189 11. *C. Alt et al.* [NA49 collaboration] Energy dependence of Λ and Ξ pro-
190 duction in central Pb + Pb collisions at 20A, 30A, 40A, 80A, and 158A
191 GeV measured at the CERN Super Proton Synchrotron // Phys. Rev.
192 C — 2008. — V. 78. — P. 034918.
- 193 12. *L. Ahle et al.* [E802 collaboration] Particle production at high baryon
194 density in central Au+Au reactions at 11.6A GeV/c // Phys. Rev. C —
195 1998. — V. 57. — P. R466-R470.
- 196 13. *P. Chung et al.* [E895 collaboration] Near-Threshold Production of
197 the Multistrange Ξ^- Hyperon // Phys. Rev. Lett. — 2003. — V. 91. —
198 P. 202301.
- 199 14. *M.I. Abdulhamid, B.E. Aboona et al.* [STAR collaboration] Strangeness
200 production in $\sqrt{s_{NN}} = 3 \text{ GeV}$ Au+Au collisions at RHIC // J. High Energ.
201 Phys. — 2024. — V. 10. — P. 139.

- 202 15. *M.S. Abdallah, B.E. Aboona et al.* [STAR collaboration] Probing
203 strangeness canonical ensemble with K^- , $\phi(1020)$ and Ξ^- production in
204 Au+Au collisions at $\sqrt{s_{NN}} = 3$ GeV // Phys. Lett. B — 2022. — V. 831. —
205 P. 137152.
- 206 16. *Linnyk, O.* and *Bratkovskaya, E. L.* and *Cassing, W.* Strangeness pro-
207 duction within parton–hadron–string dynamics (PHSD) // J. Phys. G:
208 Nucl. Part. Phys — 2010. — V. 37. — P. 094039.
- 209 17. *Jahan, H.* and *Ahmad, S.* Multi-Strange production at FAIR energy. //
210 PoS — 2017. — V. ICPAQGP2015. — P. 051.